JOURNAL OF APPLIED POLYMER SCIENCE VOL. 17, PP. 1253–1268 (1973)

Gel Permeation Chromatography: Physical Characterization and Chromatographic Properties of Porasil*

A. R. COOPER† *Department of Pure and Applied Chemistry, Thomas Graham Bldg., University of Strathclyde, Glasgow, Scotland,* and EDWARD M. BARRALL II, *IBM Research Laboratory, Monterey and Cottle Roads, San Jose, California 95114*

Synopsis

Porasil** porous silica has been characterized by the methods of gas adsorption–desorption isotherms, mercury porosimetry, and electron microscopy. The pore structure has been shown to be quite heterogeneous, particularly at the surface of the particles. From the same sample of Porasil, columns were packed and calibrated in a gel permeation chromatograph. The availability of high molecular weight fractions of polystyrene allowed the exclusion limit of these materials to be determined for the first time. The heterogeneous pore structure did not seem to affect the effectiveness of these materials for macromolecular separation.

INTRODUCTION

The use of porous silica beads for a column packing in gel permeation chromatography (GPC) was first reported by de Vries et al.[1] Calibration curves were presented for four silica substrates, using polystyrene solutes having molecular weights between 10^4 and 10^6 and tetrahydrofuran solvent. Later, de Vries et al.[2] reported the use of six Porasil substrates, coded A through F, using polystyrene and poly(vinyl chloride) solutes in tetrahydrofuran and additionally polydextran solutes in water. For aqueous use, 1% diethylene glycol was added to suppress adsorption effects. Average pore diameters determined by mercury porosimetry and BET surface areas were reported. Bombough et al.[3] reported a deactivated Porasil which could be used directly with water as solvent to elute polydextrans and poly(vinyl alcohols). Porasil substrates A through F are now distributed by Waters Associates,[4] and the calibration curves for these, using polystyrene solutes having molecular weights $10^2 \rightarrow 2 \times 10^6$ in toluene,

* Part II of a Series on Characterization and Properties of Macromolecules.

† Present address: Department of Chemistry and Institute of Materials Science, University of Connecticut, Storrs, Connecticut 06268.

** Porasil is the Water Associates registered trademark for a powdered porous silica chromatographic substrate.

have been published by Kelley and Billmeyer.[5] Deactivation of Porasil using N-O-bis(trimethylsilyl)acetamide has been described.[6] Electron micrographs of crushed samples of Porasil have been reported[7] and showed that each bead is a three-dimensional network of interconnected pores.

There is, however, no information available in the literature where the detailed characterization of the porous structure of the various Porasil substrates has been determined for the same samples used for obtaining the GPC calibration curves. We have used the methods of electron microscopy, mercury porosimetry, and low-temperature nitrogen adsorption to characterize the six available Porasil substrates. Additionally, with the same samples the calibration curves for each of these substrates have been determined using polystyrene solutes in the molecular weight range 9×10^2 to 8.8×10^6 and toluene solvent. The substrates were treated with hexamethyldisilazane[8] to eliminate adsorption by refluxing in *n*-hexane for 6 hr.

EXPERIMENTAL

The physical methods used to characterize these porous silica materials have been described in detail previously.[9]

RESULTS AND DISCUSSION

The results obtained from nitrogen adsorption measurements and mercury porosimetry for the surface areas and pore volumes of the six Porasil packings are shown in Table I. The manufacturers quote values for the surface area only. The results obtained here for the surface area, using the full BET analysis, differ considerably from the quoted values.

TABLE I
Pore Volumes and Surface Areas of Porasil Column-Packing Materials

Sample designation	Surface area manufacturer's values, m^2/g	BET surface area, m^2/g	Liquid nitrogen micropore volume,[a] cc/g	Mercury pore volume, cc/g		
				Total	Micropore volume[b]	Macropore volume[c]
Porasil 2000+	1.5	—	—	0.477	0.095	0.382
Porasil 1500	4	13.5	—	0.710	0.228	0.481
				(0.720)	(0.232)	(0.488)
Porasil 1000	25	30.9	—	0.762	0.723	0.039
				(0.795)	(0.749)	(0.046)
Porasil 400	50	82.9	0.874	0.947	0.928	0.019
Porasil 250	200	137.6	0.925	0.818	0.804	0.015
Porasil 60	480	519.9	1.034	0.751	0.738	0.012

[a] Pore volume having pore radii below 500 Å.
[b] Pore volume having pore radii between 22 and 500 Å.
[c] Pore volume having pore radii between 500 and 5020 Å.

The surface area of Porasil 2000 was not determined because with such a small surface area the use of nitrogen adsorption is not suitable for accurate measurements. The pore volumes of these materials are high, comparable with the porous glass manufactured by Corning.[9] The liquid nitrogen micropore volume measures the volume of the pores having radii of 500 Å or less. The mercury pore volume measures the pore volume having the pore radii between 22 and 5020 Å (these values depend on the values chosen for the contact angle of mercury on silica and the surface tension of mercury). This mercury pore volume can also be divided at 500 Å pore radius into a mercury micropore volume and a mercury macropore volume. For Porasil 60 and Porasil 250, the micropore volume from the nitrogen adsorption is greater than that from mercury porosimetry. This is most probably due to the presence of pores in each sample smaller than 22 Å, the lower limit of the mercury porosimetry method. For Porasil 400, the agreement in the micropore volumes determined by both methods is within 6%. The pore volume of Porasil 2000+ is considerably lower than the others.

The differential pore volume distributions DPVD of these materials determined by mercury porosimety measurements are shown in Figures 1 to 3, and those from nitrogen desorption measurements, in Figure 4. The values of the radii at the peak of the DPVD are recorded in Table II together with the width of the distribution, obtained by measuring the width at the base of the DPVD where the tangents to the curve cross.

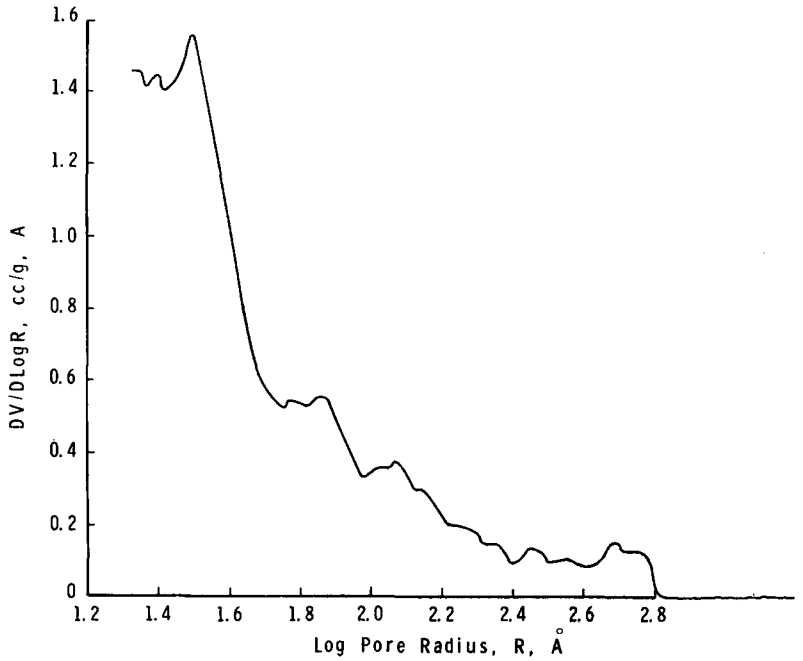

Fig. 1. Differential pore volume distribution of Porasil 60 by mercury porosimetry.

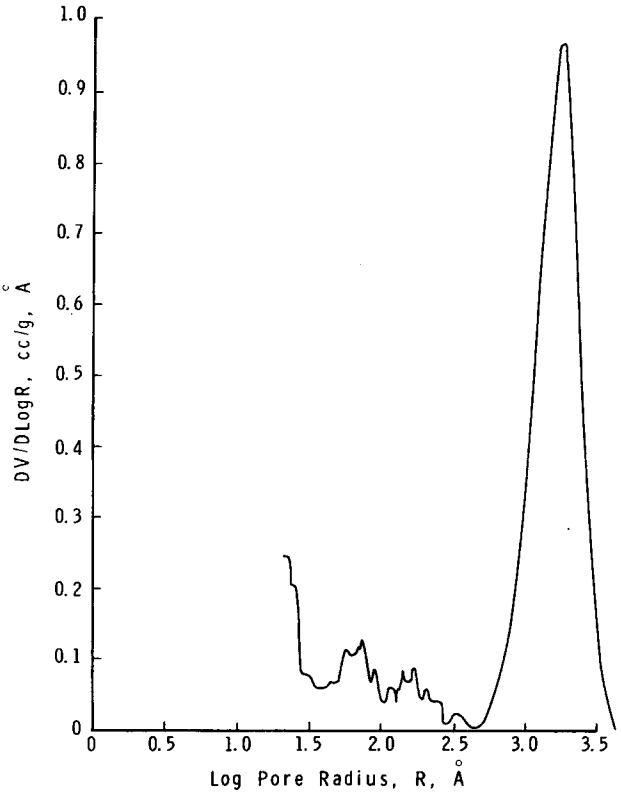

Fig. 2. Differential pore volume distribution of Porasil 2000+ by mercury porosimetry.

The values of the integral pore volume at which these two values of the pore radii occur are quoted in parentheses in the table. With the exception of Porasil 2000, the main peak in the DPVD contains 85–90% of the total pore volume. Porasil 2000 has a particularly broad pore size distribution in the main peak and also has 27% of its pore volume outside of this range. Porasil 60, 250, and 400 are amenable to pore size distribution analysis by both mercury porosimetry and nitrogen desorption isotherm techniques. The agreement between the two methods for the value of the radii at the maximum in the DPVD is extremely good for all three samples. For Porasil 250 and 400, the agreement on the width of the distribution is also good. The width of the distribution for Porasil 60 could not be determined fully by mercury porosimetry. The average pore radius calculated from (2 × pore volume)/surface area, which assumes cylindrical shaped pores, is generally larger than the radius determined from the maximum in the DPVD.

The widths of the pore size distribution are greater for Porasil than for Corning porous glasses.[9] However, the average pore sizes of Porasil extend over a wider range of pore radius and are thus useful for separating over a wider range, particularly at lower molecular weights.

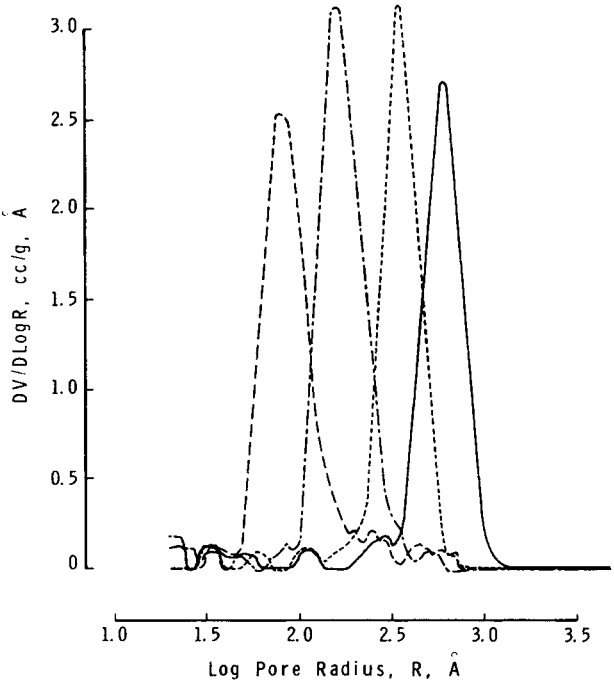

Fig. 3. Differential pore volume distributions of Porasil 250, 400, 1000, and 1500 by mercury porosimetry: (– – – –) Porasil 250; (- - - - -) Porasil 400; (- - - - - - - -) Porasil 1000; (———) Porasil 1500.

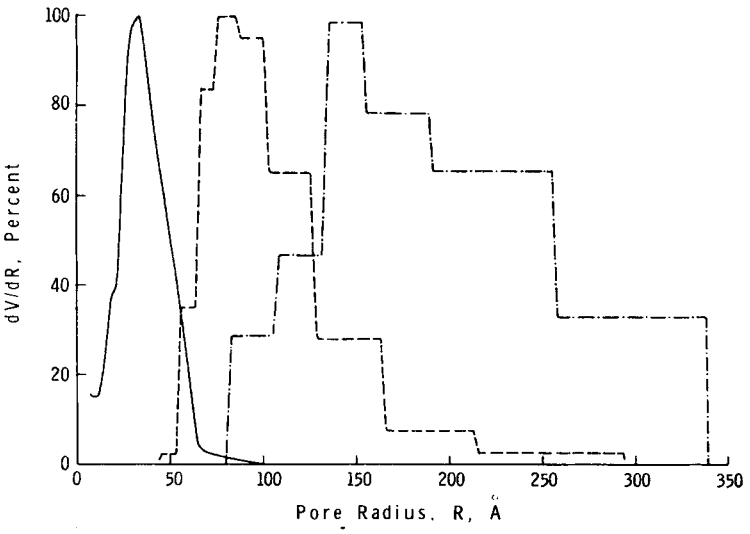

Fig. 4. Differential pore volume distributions of Porasil 60, 250, 400 by nitrogen desorption isotherms: (·—·—) Porasil 400; (– —) Porasil 250; (———) Porasil 50.

TABLE II
Differential Pore Volume Distributions, DPVD, of Porasil Column Packing Materials

Porasil designation	Nitrogen desorption isotherms				Mercury porosimetry			
	Average micropore radius,[a] Å	Pore radius at maximum in DPVD, Å	Pore radii at base of DPVD, Å		Average pore radius,[b] Å	Pore radius at maximum in DPVD, Å	Pore radii at base of DPVD,[c] Å	
2000+ (F)	—	—	—	—	—	1780	3354 (5%)	751 (78%)
1500 (E)	—	—	—	—	1052	596	945 (2%)	376 (87%)
					1066	563	945 (1%)	376 (87%)
1000 (D)	—	—	—	—	493	335	563 (2%)	224 (90%)
					514	316	563 (3%)	244 (87%)
400 (C)	211	145	330	80	229	159	299 (5%)	100 (94%)
250 (B)	134	85	175	50	119	80	141 (14%)	50 (97%)
60 (A)	40	35	63	17	—	32	—	—

[a] Calculated from 2 × nitrogen micropore volume/BET surface area.
[b] Calculated from 2 × mercury pore volume/BET surface area.
[c] Values in parentheses indicate the percentage integral pore volume at which the quoted radii occur.

The method of mercury porosimetry is not capable of detecting large voids inside a porous sample as the whole void fills with mercury when the largest opening to the surface of the bead is being penetrated with mercury. For this reason, the Porasil column packing materials were examined in the electron microscope.

Electron Microscopy

Samples of each pore size group of Porasil were embedded in epoxy resin and sliced into 800-Å-thick sections (by interference color) with an Ultratome II ultramicrotome equipped with a diamond knife. This technique has been described in detail elsewhere.[10] After mounting the thin sections on carbon-coated grids and overcoating them with carbon, they were examined in a Japan Electron Optics J.E.M. 6-A electron microscope at an 80-kV beam voltage. The micrographs were recorded on Kodak medium projector slide glass plates. Magnification was calibrated by the diffraction grating technique. At all stages in sample manipulation, care was exercised to avoid crushing or cracking the glass structure. The figures presented in this study are positive prints of the plates. Thus, the dark areas are the electron-opaque areas (glass), and grey areas are the pores. In the small pore-size samples, several layers of pores overlap, giving a highly shaded picture. From these, a general idea of pore types may be obtained, but measurement is not possible.

The electron micrographs indicate a fundamental difference in structure between Porasil and other porous media observed in our previous studies.[9-11] Within a given chip of relatively uniform pore distribution are islands of very small pore diameter. In addition, some chips of Porasil 1500 are *coated* with smaller pore-size material. Examples of this inclusion and coating are shown in Figures 5 and 6. A large number of voids were also noted in other pore size ranges. These voids are clearly evident in Figure 5.

The presence of both very much larger and very much smaller pores in a given sample agrees well with the differential pore volume studies. The small peaks present in each sample (see Fig. 3) on both sides of the average are the result of this polydispersity. However, this polydispersity in no way resembles that reported previously for a sample of Bio-Glas of intentionally broad pore distribution.[11] The pore size groups in Porasil are sharply defined, not a continuous gradation.

Figure 7 shows a section taken in the middle of a Porasil 2000+ chip. The average pore distribution by geometric measurements is 2500 Å radius. This is very near the *average* calculated from the maximum and base of the mercury porosimetry data given in Table II. The light areas in the micrograph are regions where the epoxy medium did not completely adhere.

Figure 8 shows an edge of a Porasil 1500 chip. The extensive regions of very small pore size are obvious. A few large void volumes appear in the interior of the chip. The heterogeneous nature of the individual chips results in the anomalous pore radii calculations given in Table II.

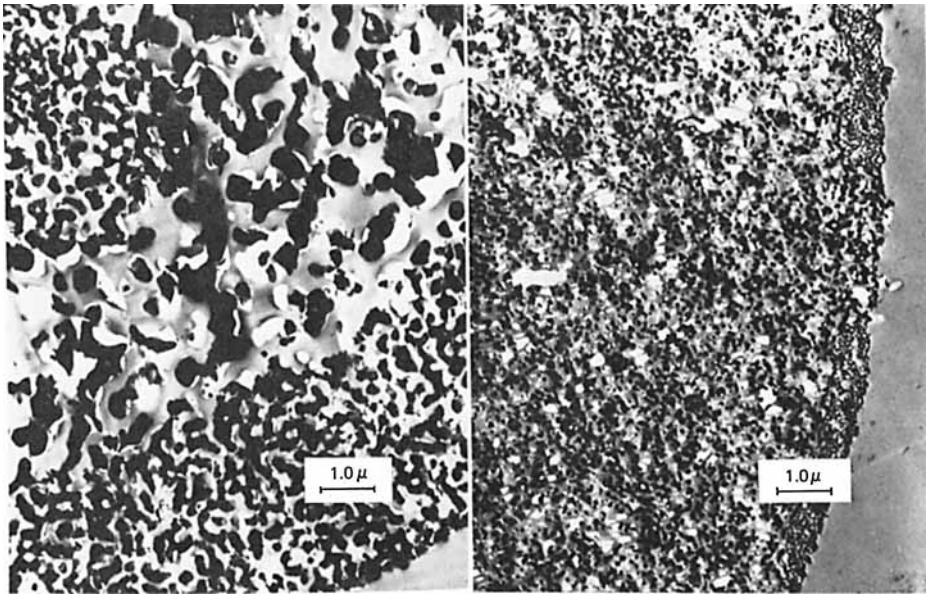

(a) (b)

Fig. 5. Electron micrographs showing the heterogeneous pore structure of Porasil 2000 and 1500: (a) Porasil 2000 10,000×; (b) Porasil 1500 10,000×.

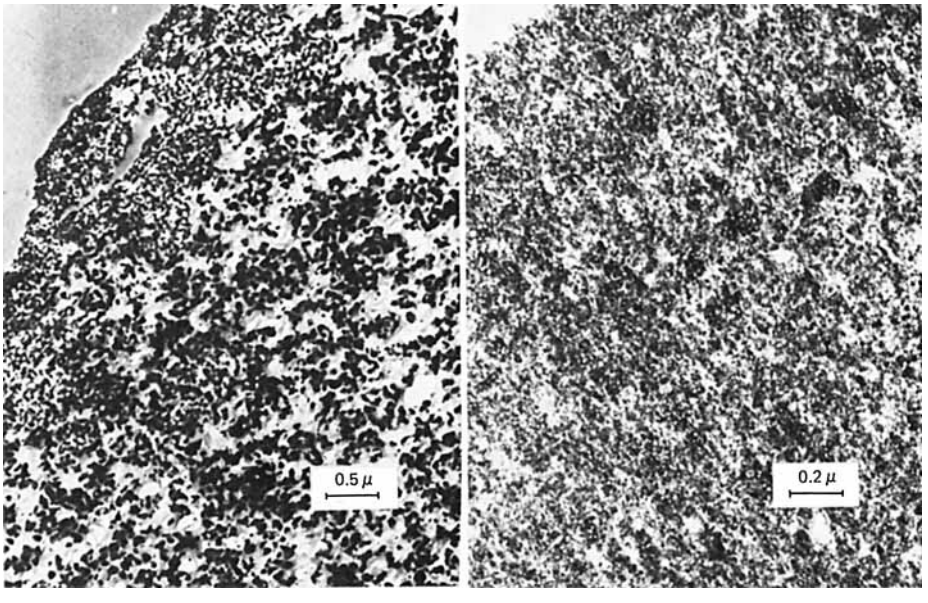

(a) (b)

Fig. 6. Electron micrographs showing the heterogeneous pore structure and void distribution in Porasil 400 and 250: (a) Porasil 400 20,000×; (b) Porasil 250 50,000×.

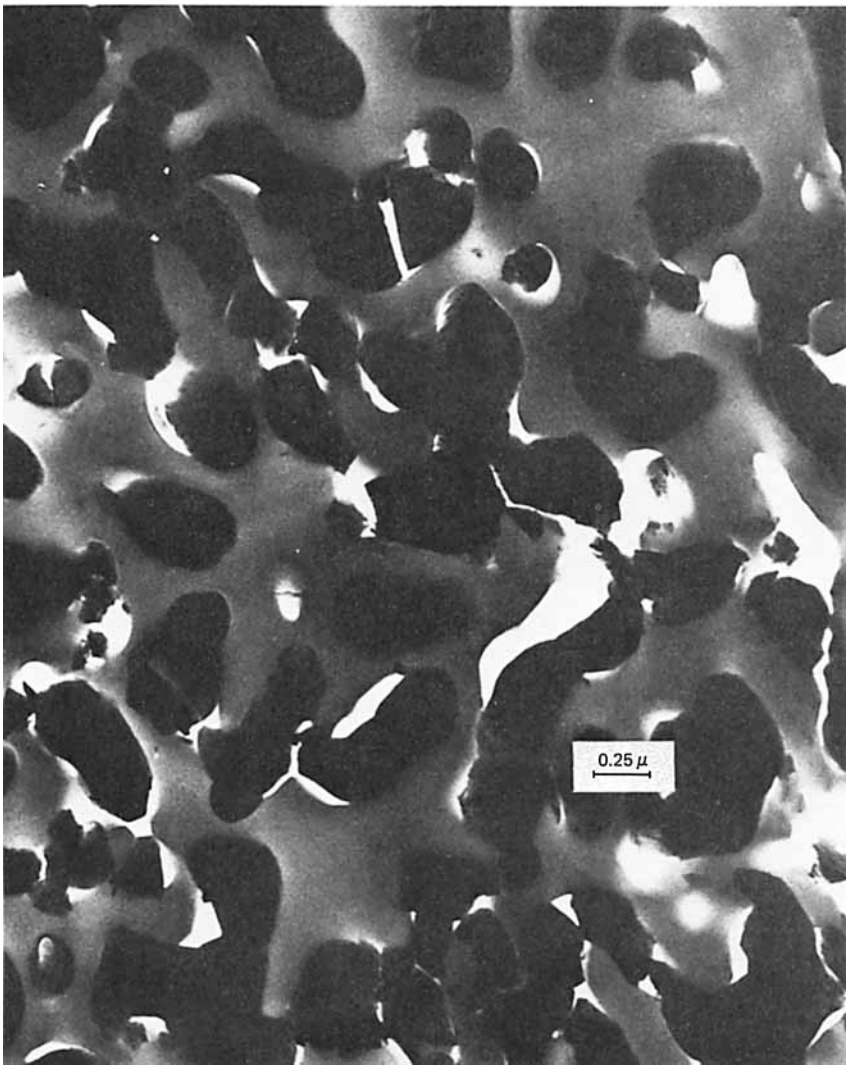

Fig. 7. Electron micrograph of Porasil 2000 at 40,000×.

Porasil 1000 (Fig. 9) has a large number of internal voids. Several fields, of which Figure 9 is a good representative, had as much as 10% of the pores in the form of internal voids with diameters greater than 3000 Å. However, very small pores were almost completely absent.

Figure 10 shows the relatively uniform texture characteristic of Porasil 400. Large void volumes are evident but not significantly represented in ten fields studied. The same is true of Porasil 250, Figure 11, and 60, Figure 12. The smaller pore-size material is far more uniform within a chip than the larger material. Variation from chip to chip is large. From our observations, there appear to be *two pore-size* chips in each of the groups represented as 400, 250, and 60.

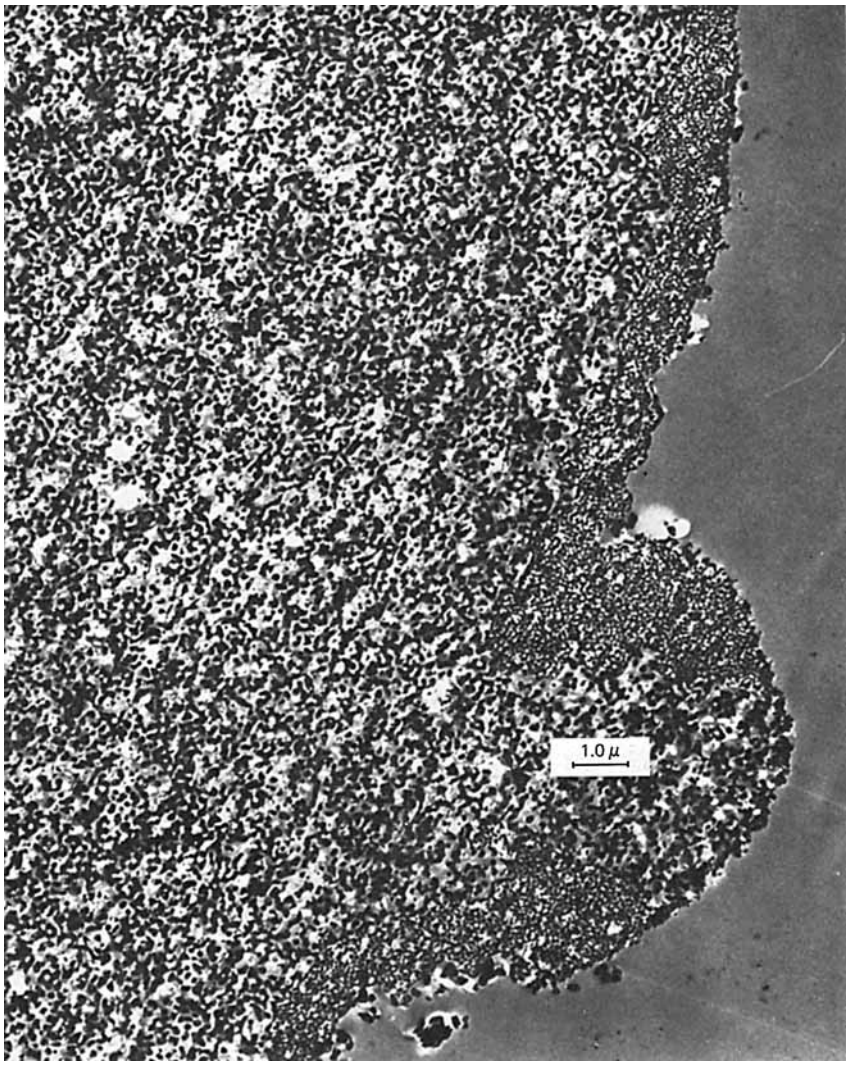

Fig. 8. Electron micrograph of Porasil 1500 at 10,000×.

In general, the Porasil samples are relatively polydisperse with respect to pore sizes. The efficiency of the larger pore sizes may suffer due to entrapment of large molecules in a chip half of which is covered by a layer of small pore-size material. The numerous very large void volumes within chips could have the same effect. The electron micrographs published by de Vries do not show these features.[7] This could be ascribed to two reasons: (1) the de Vries samples were not identical to the commercial Porasil; and (2) the de Vries samples were prepared by crushing to very small particle size. Crushing could result in selective cracking along pore boundaries and the destruction or dilution of heterogeneous features.

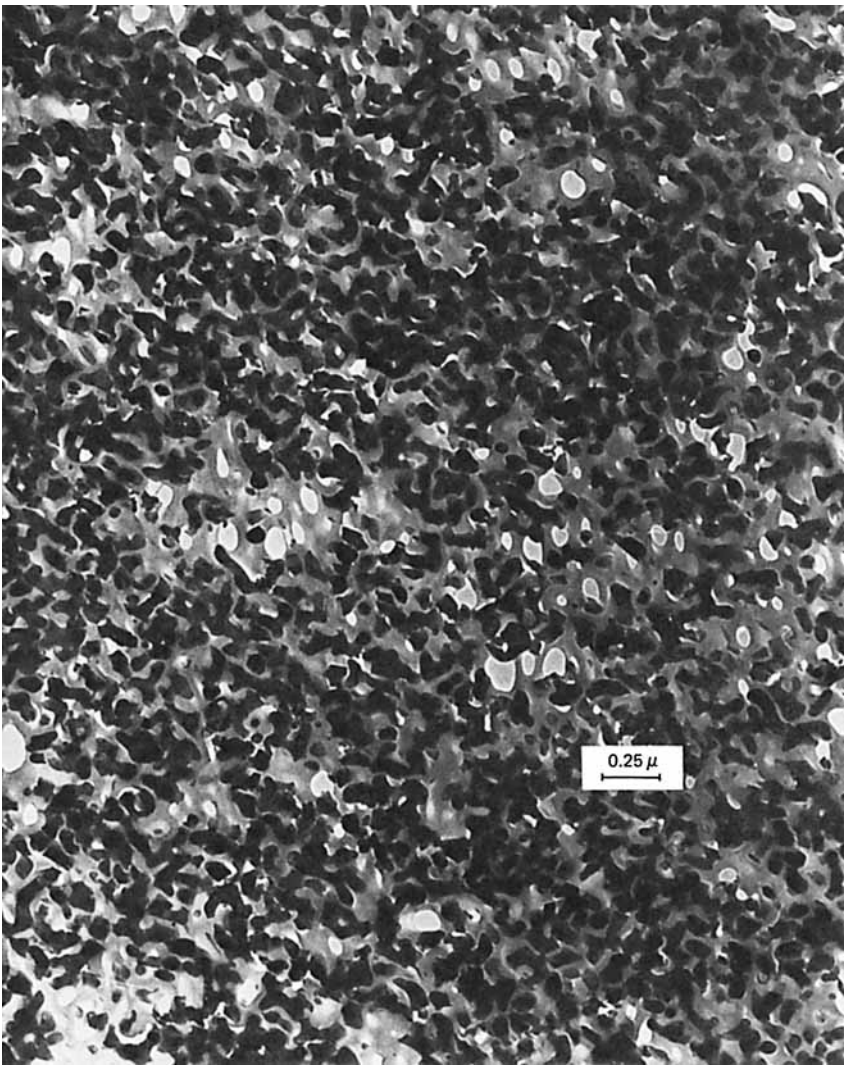

Fig. 9. Electron micrograph of Porasil 1,000 at 40,000×.

Thin sections where the whole chip is preserved in section avoids this problem. The present electron microscope evidence serves to support and clarify in detail the data reported in Table II.

Gel Permeation Chromatography

GPC calibration curves were obtained for each Porasil sample using polystyrene solutes dissolved in toluene (concentration 1.0 mg/ml) and a standard column 4 ft in length and 0.305 in. I.D. The instrument used was an ANA-PREP operating at room temperature, and the flow rate was 2.4 ml/min. The polystyrenes used were commercially available, anioni-

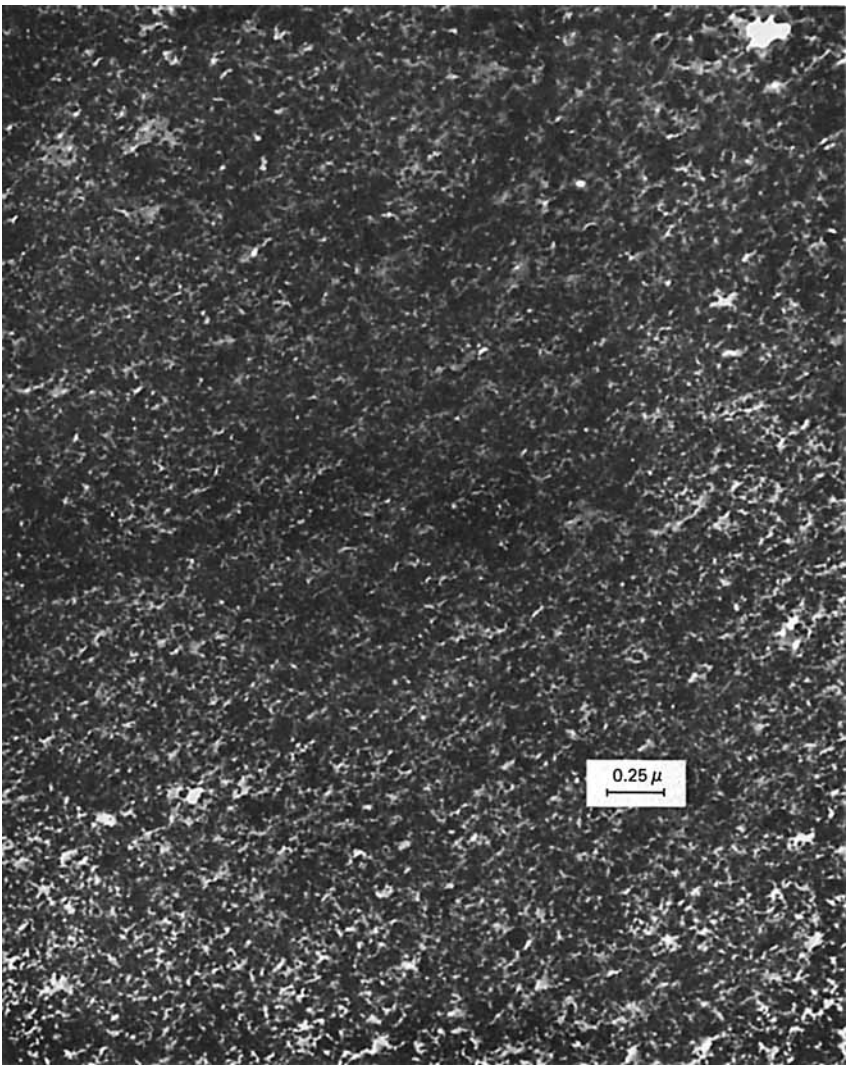

Fig. 10. Electron micrograph of Porasil 400 at 40,000×.

cally polymerized samples except for the sample having $M_{\bar{w}} = 8.87 \times 10^6$ (determined by light scattering) which was fractionated from a styrene sample which had polymerized at room temperature for several years. The calibration data for the Porasil-packed columns are shown in Table III and are plotted in Figure 13. From the figure the useful separating range for these column packing materials may be evaluated; these are tabulated in Table IV.

Figure 13 shows the calibration curve for these six Porasil columns connected in series with polystyrene solutes and toluene solvent flowing at 2.40 ml/min. The column inlet pressure required to attain this flow rate

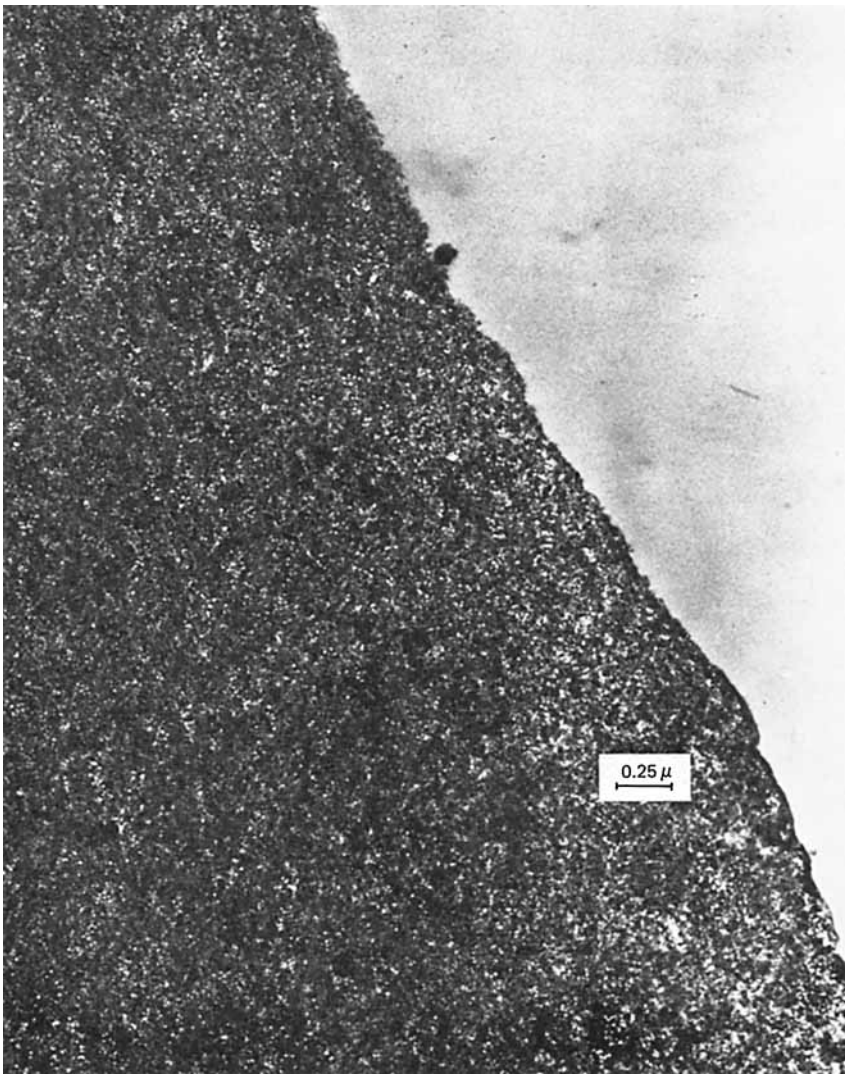

Fig. 11. Electron micrograph of Porasil 250 at 40,000×.

was 100 psi, which is considerably less than that required for a similar bank of polystyrene gel columns. The curve is very similar to that found previously for a series combination of columns packed with Corning porous glass,[9] and the range spans that of most commercial polymers. The curved portions of the curve at either end could be linearized by adding further columns packed with Porasil 2000+ or Porasil 60. A plate count for the six columns in series using hexane as the test solute indicated 60 plates/ft. This is smaller than the value of 117 plates/ft found for the series combination of columns packed with Corning glass. In the latter case, the porous structure was much more uniform than that found here for

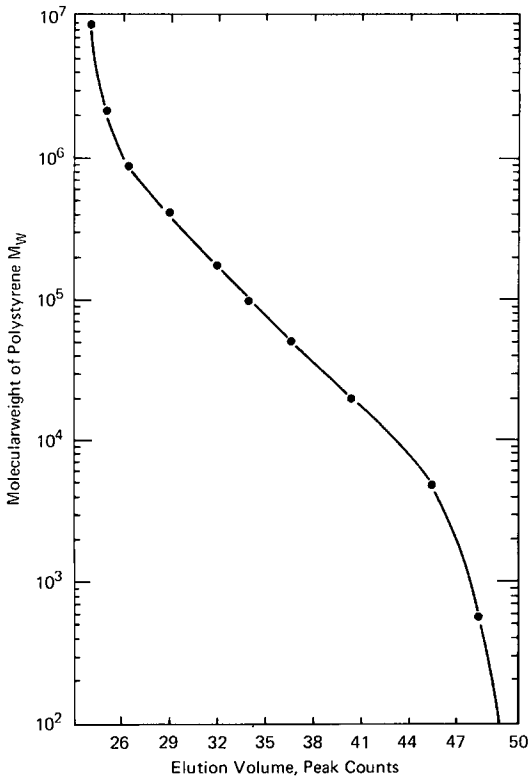

Fig. 12. GPC calibration curves for Porasil packed columns for polystyrene solutes and toluene solvent at room temperature.

TABLE III
Elution Volume Data for Porasil Packed Columns with Polystyrene Solutes and Toluene Solvent[a]

Polystyrene M_w	Porasil 2000+	1500	1000	400	250	60
8.87×10^6	5.41	5.32	5.26			
2.145×10^6	6.53	5.48	5.28	5.12		5.18
8.67×10^6	7.51	5.64	5.37	5.18	5.47	
4.11×10^5	8.32	6.66	5.64		5.45	5.18
1.73×10^6	8.84	8.13	6.85	5.56	5.60	
9.82×10^4	9.00	8.49	7.56	6.19	5.70	
5.1×10^4	9.14	8.84	8.27	7.18	6.17	
1.98×10^4			8.90	8.4	7.32	5.35
1.03×10^6	9.37	9.13	9.26	9.0	8.14	5.76
5×10^3	9.42		9.40	9.47	8.87	
2×10^3					9.29	7.40
600	9.45		9.65	9.86	9.52	8.26
n-Hexane	9.46	9.79	9.82	10.11	10.12	9.47
Plates/ft[b]	130	78	212	189	102	151

[a] Values reported are peak counts which are, at this flow rate, equal to 5.37 ml.

[b] Plates per foot (n) calculated from hexane elution volume (V_e) and peak width at the base (W_b) via $n = 1/L(V_e/W_{b/4})^2$, where L is the column length in feet.

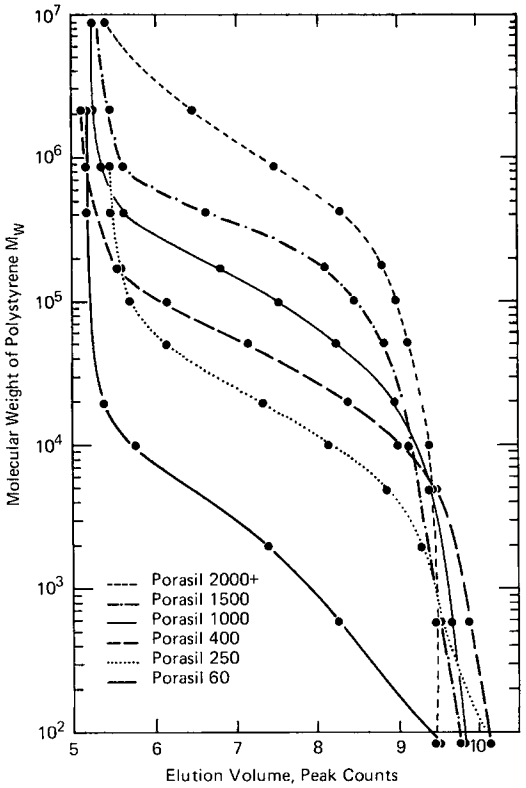

Fig. 13. GPC calibration curve for six Porasil packed columns connected in series for polystyrene solutes and toluene solvent at room temperature.

the Porasil samples. A detailed analysis of results obtained using columns packed with polystyrene gels, Corning porous glasses, and Porasils, and a comparison of their relative efficiencies is in preparation.

The heterogeneous nature of the pore structure found here for Porasil materials would preclude its use for studying theoretical proposals relating polymer elution characteristics to pore size dimensions. This pore struc-

TABLE IV
Useful Separating Ranges of Porasil Substrates in GPC

Porasil[a]	Useful range for polystyrenes in toluene
2000+ (F)	$9\times10^7 \rightarrow 2\times10^5$
1500 (E)	$1\times10^6 \rightarrow 5\times10^4$
1000 (D)	$4\times10^5 \rightarrow 2\times10^4$
400 (C)	$2\times10^5 \rightarrow 5\times10^3$
250(B)	$1\times10^5 \rightarrow 2\times10^3$
60 (A)	$2\times10^4 \rightarrow 80$

[a] An alphabetic designation has been used for Porasil. The relationship between the numerical and alphabetic systems are given here.

ture does not obviate its use as a GPC column packing material for the determination of molecular weight distributions.

References

1. A. J. de Vries, M. LePage, R. Beau, and C. L. Guillemin, *Anal. Chem.*, **39**, 935 (1967).

2. M. LePage, R. Beau, and A. J. de Vries, *J. Polym. Sci. C.*, **21**, 119 (1968).

3. K. J. Bombaugh, W. A. Dark, and J. N. Little, *Anal. Chem.*, **41**, 1337 (1969).

4. Waters Associates, Framingham, Mass.

5. R. N. Kelley and F. W. Billmeyer, *Anal. Chem.*, **42**, 399 (1970).

6. F. A. Sliemers, K. A. Boni, D. E. Nemzer, and G. P. Nance, Preprints of Sixth International Seminar on Gel Permeation Chromatography, Miami Beach, Florida, 1968, p. 463.

7. R. Beau, M. LePage, and A. J. de Vries, Proceedings of the International Symposium on Polymer Characterization, Battelle Memorial Institute, Columbus, Ohio (Nov.–Dec. 1967), *Appl. Polym. Symposia*, **8**, 137 (1969).

8. A. R. Cooper and J. F. Johnson, *J. Appl. Polym. Sci.*, **13**, 1487 (1969).

9. A. R. Cooper, A. R. Bruzzone, J. H. Cain, and E. M. Barrall II, *J. Appl. Polym. Sci.*, **15**, 571 (1971).

10. E. M. Barrall and J. H. Cain, *J. Polym. Sci. C*, **21**, 253 (1968).

11. E. M. Barrall, J. H. Cain, and A. R. Cooper, in *Gel Permeation Chromatography*, K. Altgelt and L. Segal, Eds., M. Dekker, New York (1971), p. 165.

Received June 29, 1972